J Electroceram (2006) 17:205–209
DOI 10.1007/s10832-006-8318-5

Structure and magnetic properties of R-P phase $Sr_3Mn_{2-x}Fe_xO_{7-\delta}$ ($0.10 \leq x \leq 0.5$)

Jin Hyun Shin · Min Seok Song · Jai Yeoul Lee*

Received: 15 July 2005 / Revised: 21 February 2006 / Accepted: 16 March 2006

Abstract Double layer R-P (Ruddlesden-Popper) manganate phases were stabilized in an air atmosphere by partial substitution of Mn by Fe. The crystal structures and magnetic structures of the R-P phase $Sr_3Mn_{2-x}Fe_xO_{7-\delta}$ ($x = 0.1$, 0.2, and 0.5) have been refined from the room temperature and low temperature neutron diffraction data.

All of these samples adopt space group I4/mmm at room temperature. 10 K diffraction patterns showed antiferromagnetic ordering and magnetic superlattice reflection pattern that can be indexed on a $2a_0 \times 2a_0 \times c_0$ supercell for $x = 0.1$ and $x = 0.2$ samples. The temperature dependence of the ZFC (zero field cooled) and FC (field cooled) molar magnetic susceptibility curve showed divergence for $x = 0.5$ samples which implies that this double R-P phase shows spin-glass transition.

Keywords Double layer R-P manganate · Crystal structure · Neutron diffraction · Magnetic susceptibility · Spin glass

1 Introduction

The manganates with perovskite structure, $Ln_{1-x}A_xMnO_3$ (Ln = rare earth ion, A = alkali or alkaline earth metal ion) have been extensively studied due to their magnetotransport properties such as colossal magnetoresistance (CMR) [1–3]. Recently layered perovskite manganates also received considerable attention since the observation of the CMR properties in R-P (Ruddlesden-Popper) phase $La_{1+x}Sr_{2-x}Mn_2O_7$ [4–7]. CMR phase $La_{1+x}Sr_{2-x}Mn_2O_7$ is a typical R-P phase with $n = 2$ in general formula $(AO)(AMO_3)_n$, where the perovskite structure is the $n = \infty$ end member. The $n = 2$ R-P phase, Fig. 1, can be thought as of double layers of MO_6 octahedra along the c-axis separated by an insulating rock-salt layer (AO).

The parent compound of the $n = 2$ CMR manganate $Sr_3Mn_2O_{7-\delta}$ was synthesized by quenching the sample from 1650°C into dry ice by Mitchell et al. [8, 9]. This phase contains a large number of oxygen vacancies and is an antiferromagnetic insulator with $T_N = 160$ K. A series of Mn substituted R-P strontium ferrate were prepared and their structure and magnetic properties were reported by Veith et al. [10].

The oxygen deficient double layer perovskite $Sr_3Mn_2O_6$ phases were synthesized in N_2 atmosphere and its structure and properties are reported by Gillie et al. [11]. TEM experiment showed that this phase crystallized in a superstructure of the simple R-P subcell. Magnetic susceptibility studies suggested a canted antiferromagnetic transition and showed no divergence between ZFC and FC curves.

Recently double layer R-P phase $Sr_3Mn_{2-x}Fe_xO_{7-\delta}$ stabilized at room temperature in air atmosphere its room temperature crystals structure and properties are reported [12]. The X-ray diffraction experiment showed that this phase crystallized in a space group I4/mmm.

In this study, crystal and magnetic structure analysis of double layer R-P manganate phases, $Sr_3Mn_{2-x}Fe_xO_{7-\delta}$ were carried out by neutron diffraction data and magnetic properties are discussed in detail.

J. H. Shin · M. S. Song · J. Y. Lee (✉)
Department of Materials Science and Engineering,
Center for Materials Research Yeungnam University, 214-1
Daedong Gyongsan Gyoungbuk, 712-749, Korea
e-mail: jylee@yu.ac.kr

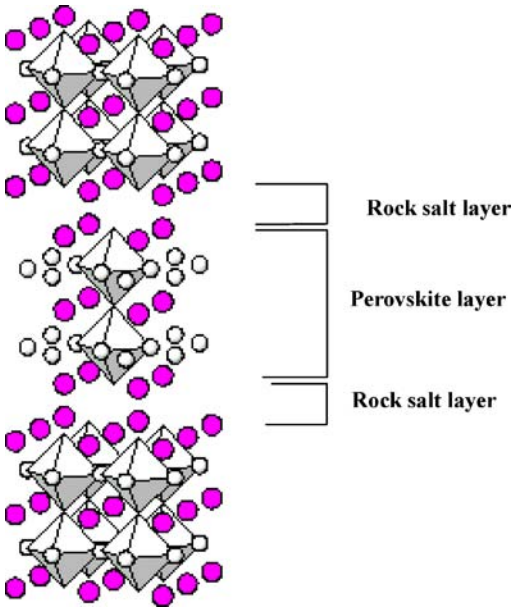

Fig. 1 The $n = 2$ Ruddlesden-Popper structure

2 Experimental

Polycrystalline phases of $Sr_3Mn_{2-x}Fe_xO_{7-\delta}$ were prepared by conventional solid state reaction of $SrCO_3$, MnO_2, and Fe_2O_3 (99.9%, Aldrich). The powder mixture was pressed into a pellet and heated at 1350 to 1500°C for 48 h in air atmosphere, with intermediate grindings. Phase analysis of the products was carried out by X-ray powder diffraction. Neutron diffraction data were recorded over the temperature range of 5–300 K on the high resolution powder diffractometer (HRPD) at KAERI (Korea Atomic Energy Research Institute), Korea. Rietveld structural refinements were carried out with the FullProf program package [13]. Magnetic susceptibility curves of the samples were obtained using a Quantum Design SQUID magnetometer over the temperature range of 5–300 K in an applied field of 1000 G.

3 Results and discussion

The structural parameters of double layer R-P phases $Sr_3Mn_{2-x}Fe_xO_{7-\delta}$ have been well refined by Rietveld method with room temperature neutron diffraction data on the basis of space group I4/mmm. As expected the unit cell volumes increase with the increasing Fe content due to the substitution of large Fe^{3+} for smaller Mn^{4+}. In all samples, MnO_6 octahedra show small Jahn-Teller distortions. The octahedral distortion coordinate, defined as $D = (\text{Mn-O}_{\text{apical}})/(\text{Mn-O}_{\text{equatorial}})$, is slightly increased from 1.008 for $x = 0.1$ to 1.011 for $x = 0.5$ sample at 300 K. In all samples small amount of impurity was observed in the diffraction pattern, and the affected areas were excluded from the Rietveld analysis of the data. The observed and calculated neutron diffraction pattern for $x = 0.2$ at 300 K is given in Fig. 2. The resultant structural parameters and selected bond lengths and angles at 300 K are presented in Tables 1 and 2, respectively. Neutron diffraction patterns for $x = 0.1$ and $x = 0.2$ samples revealed antiferromagnetic ordering and magnetic super reflection peaks at 10 K. The observed and calculated neutron diffraction pattern for $x = 0.2$ for magnetic structure at 10 K is given in Fig. 3. Magnetic superlattice reflections can be indexed a $2a_0 \times 2a_0 \times c_0$ supercell, where a_0 and c_0 are the unit cell dimensions of paramagnetic unit cell. The refined magnetic structure consists of an array of Mn/Fe moments

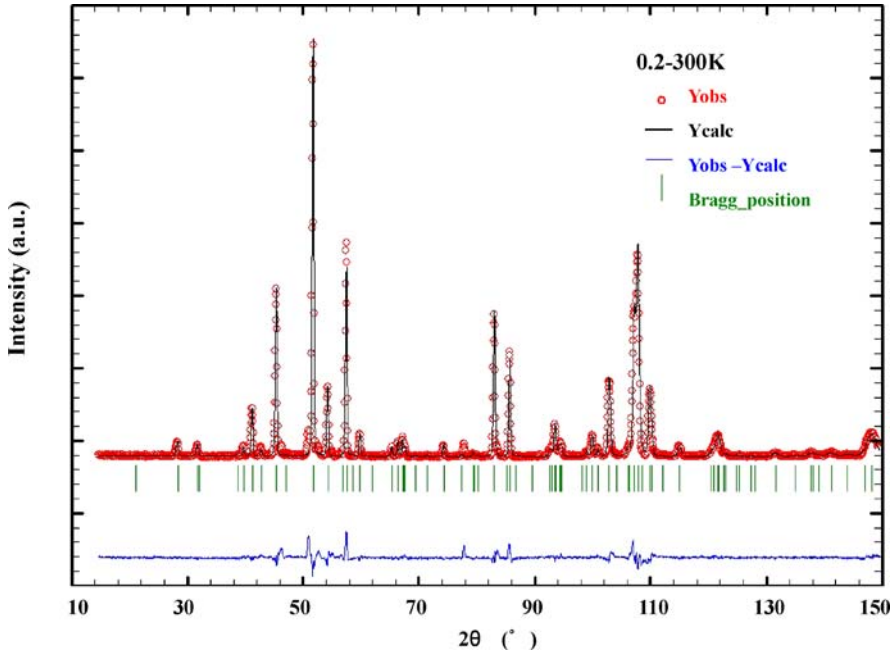

Fig. 2 Observed, calculated and difference neutron diffraction profile for $x = 0.2$ sample at 300 K. Tick marks show diffraction peak positions for nuclear structure

Table 1 Structural parameters of $Sr_3Mn_{2-x}Fe_xO_{7-\delta}$ at 300 K

	$x = 0.1$	$x = 0.2$	$x = 0.5$
a (Å)	3.8109(1)	3.8184(1)	3.8297(1)
c (Å)	20.1232(9)	20.1344(9)	20.1312(8)
V (Å^3)	292.2484	293.5631	295.2562
zSr (2)	0.1834(1)	0.1836(1)	0.1829(1)
zMn/Fe	0.0963(3)	0.0956(4)	0.0973(1)
zO (2)	0.1910(1)	0.1913(1)	0.1925(1)
zO (3)	0.0951(1)	0.0947(1)	0.0944(1)
Rp	6.49	6.23	6.09
R_{wp}	9.84	8.78	8.26
R_{exp}	3.98	3.94	3.83
Chi^2	6.10	4.96	4.86

Table 2 Selected bond lengths and angles of $Sr_3Mn_{2-x}Fe_xO_{7-\delta}$ at 300 K

	$x = 0.1$	$x = 0.2$	$x = 0.5$
Mn/Fe-O1 × 1 (Å)	1.9379	1.9248	1.9588
Mn/Fe-O2 × 1 (Å)	1.9057	1.9269	1.9165
Mn/Fe-O3 × 4 (Å)	1.9056	1.9093	1.9157
O1-Mn/Fe-O2 (°)	180	180	180
O1-Mn/Fe-O3 (°)	89.27	89.46	89.25
O2-Mn/Fe-O3 (°)	90.73	90.54	91.75
O3-Mn/Fe-O3 (°)	89.99	89.99	89.95

aligned parallel to the c axis and reveals typical G-type antiferromagnetism [9, 14].

Figure 4 shows the neutron diffraction pattern for $x = 0.2$ sample recorded from 5 K to room temperature. Magnetic reflections at low angle, which are characteristics of antiferromagnetism in neutron powder diffraction patterns are almost disappeared above $T_N = 110$ K. But there was no evidence of an additional contribution from long range magnetic order for $x = 0.5$ sample. The resultant structural parameters and selected bond lengths and angles at 10 K are presented in Tables 3 and 4, respectively. The unit cell volume of the samples contract unisotropically on cooling and D parameter increases for all samples

Table 3 Structural parameters of $Sr_3Mn_{2-x}Fe_xO_{7-\delta}$ at 10 K

	$x = 0.1$	$x = 0.2$	$x = 0.5$
a (Å)	3.8013(1)	3.8089(1)	3.8207(1)
c (Å)	20.0900(1)	20.0988(1)	20.0956(1)
V (Å^3)	290.2981	291.5877	293.3505
zSr (2)	0.1833(1)	0.1835(1)	0.1831(1)
zMn/Fe	0.0959(2)	0.0955(3)	0.0956(10)
zO (2)	0.1916(1)	0.1917(1)	0.1923(1)
zO (3)	0.0952(1)	0.0947(1)	0.0943(1)
Rp	6.74	6.72	5.41
R_{wp}	10.7	9.82	7.64
R_{exp}	2.99	3.91	3.83
Chi^2	7.10	6.31	3.98

Magnetic susceptibilities of the $n = 2$ R-P phases qualitatively showed very similar behaviors with the $n = 3$ R-P phase $Sr_4Mn_{3-x}Fe_xO_{10-\delta}$ [15, 16] and the $n = 2$ R-P phase $Sr_3Fe_{2-x}M_xO_{7-\delta}$ (M = Co, Mn) [17]. The temperature dependence of the molar magnetic susceptibility and inverse magnetic susceptibility of $x = 0.2$ and $x = 0.5$ phases are shown in Fig. 5.

As the Fe content increased the Weiss constant increased from −95.2 K for the $x = 0.2$ compound to −24.3 K for the

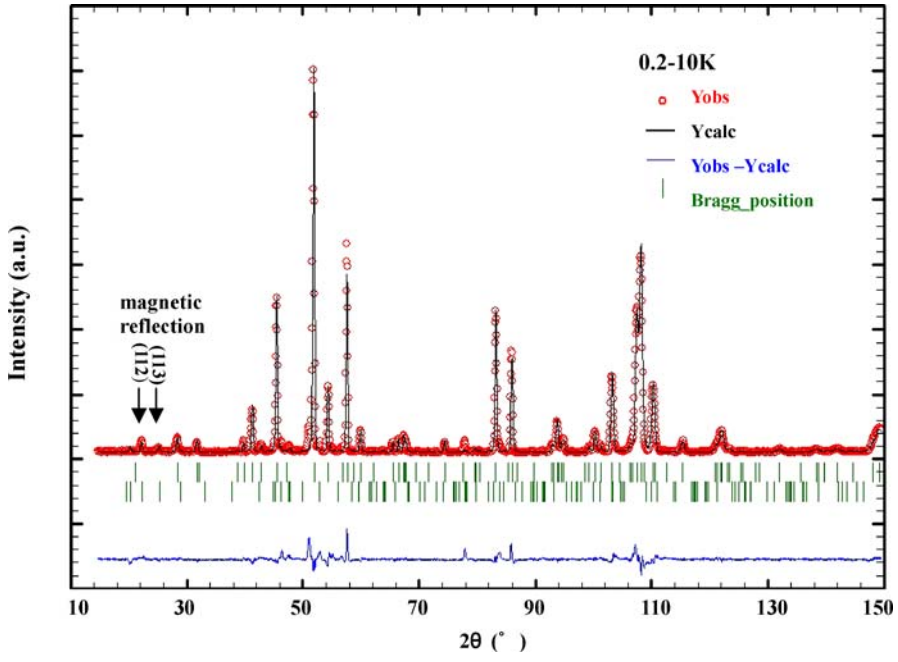

Fig. 3 Observed, calculated and difference neutron diffraction profile for $x = 0.2$ sample at 10 K. Upper tick marks represent diffraction peak positions for nuclear structure and lower tick marks are those of magnetic structure

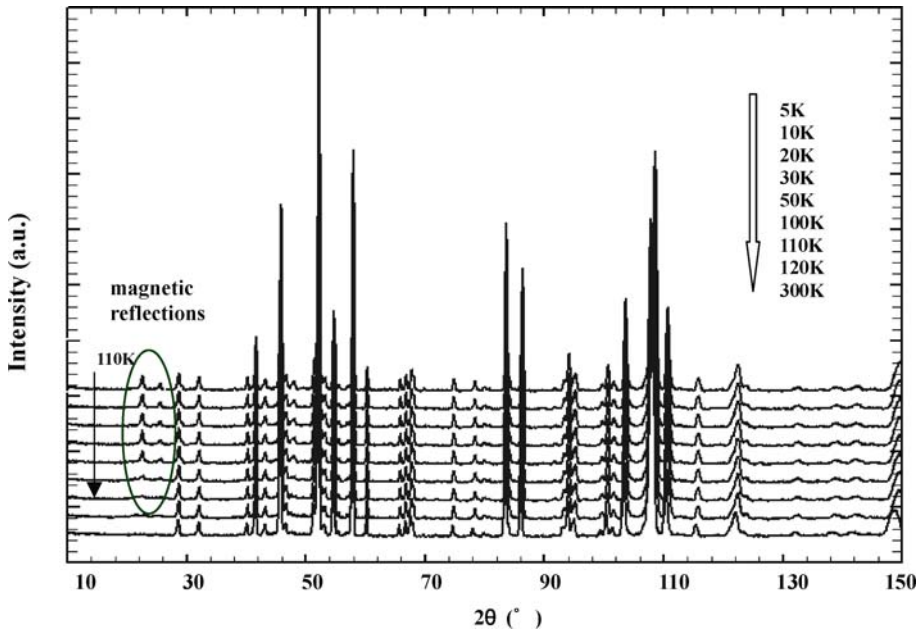

Fig. 4 Temperature dependence of the neutron diffraction pattern of $Sr_3Mn_{2-x}Fe_xO_{7-\delta}$ ($x = 0.2$). Magnetic peaks at low angle were almost disappeared at 110 K

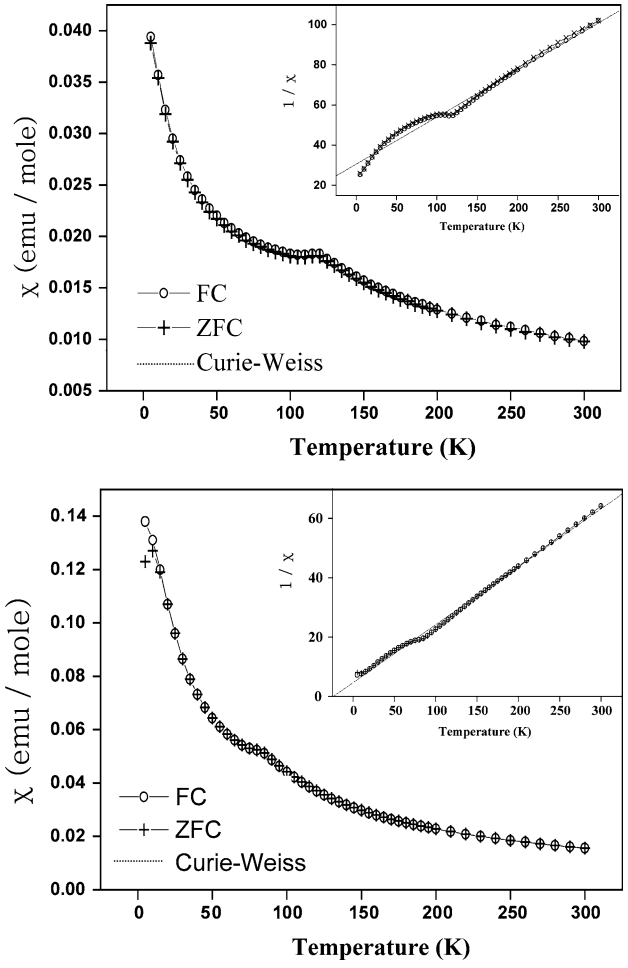

Fig. 5 The temperature dependence of the molar magnetic susceptibility and inverse magnetic susceptibility (inset) for (a) $Sr_3Mn_{1.8}Fe_{0.2}O_{7-\delta}$ and (b) $Sr_3Mn_{1.5}Fe_{0.5}O_{7-\delta}$

Table 4 Selected bond lengths and angles of $Sr_3Mn_{2-x}Fe_xO_{7-\delta}$ at 10 K

	$x = 0.1$	$x = 0.2$	$x = 0.5$
Mn/Fe-O1 × 1 (Å)	1.9266	1.9194	1.9211
Mn/Fe-O2 × 1 (Å)	1.9266	1.9335	1.9432
Mn/Fe-O3 × 4 (Å)	1.9007	1.9045	1.9105
O1-Mn/Fe-O2 (°)	179.98	180	180
O1-Mn/Fe-O3 (°)	89.58	89.52	89.22
O2-Mn/Fe-O3 (°)	90.42	90.48	90.78
O3-Mn/Fe-O3 (°)	90.00	90	89.99

$x = 0.5$ compound. The large negative value of the Weiss constant indicates that the antiferromagnetic interaction dominates in these compounds. It shows a local maximum at 110 K for the $x = 0.2$ sample which is typical of two dimensional antiferromagnetic ordering. This is also in good agreement with the previous neutron powder diffraction data shown in Fig. 4. The ZFC and FC curves showed no divergence for $x = 0.1$ and $x = 0.2$ samples. But the ZFC susceptibility curve shows maximum at 12 K, although the FC curve continues to rise slowly on further cooling for the $x = 0.5$. This means that these double R-P phase reveals spin glass transition, which is also consistent with the absence of magnetic super reflection from the neutron diffraction data collected at 10 K. This is typical of spin-glass type behavior seen in other R-P [10, 15].

4 Conclusion

The structural parameters of double layer R-P phases $Sr_3Mn_{2-x}Fe_xO_{7-\delta}$ have been refined by Rietveld method with room temperature and low temperature neutron diffraction data on the basis of space group I4/mmm.

Low temperature neutron diffraction patterns showed antiferromagnetic ordering and magnetic superlattice reflection pattern that can be indexed on a $2a_0 \times 2a_0 \times c_0$ supercell for $x = 0.1$ and $x = 0.2$ samples but not for $x = 0.5$ sample. The temperature dependence of the ZFC and FC molar magnetic susceptibility curve showed divergence for $x = 0.5$ samples which implies that this double R-P phase show spin-glass transition.

Acknowledgment This work was supported by KOSEF Grant No. M2-0411-00-0030. Authors are thanks to Dr. G. P. Hong and Dr. J. H. Park for useful discussion.

References

1. R. von Helmolt, J. Wecker, B. Holzapfel, L. Schultz, and K. Samwer, *Phy. Rev. Lett.*, **71**, 2331 (1993).
2. K. Chahara, T. Ohno, M. Kasai, and Y. Kozono, *Appl. Phys. Lett.*, **63**, 1990 (1993).
3. C.L. Canedy, K.B. Ibsen, G. Xiao, J.Z. Sun, A. Gupta, and W.J. Gallagher, *J. Appl. Phys.* **79**, 4546 (1996).
4. P.D. Battle, M.A. Green, J. Lago, J.E. Millburn, M.J. Rosseinsky, and J.F. Vente, *Chem. Mater.* **10**, 658 (1998).
5. D. Louca and G.H. Kwei, *Phys. Rev. Lett.* **80**, 3811 (1998).
6. H. Asano, J. Hayakawa, and M. Matsui, *Phys. Rev. B*, **57**, 1052 (1998).
7. N. Shah, M.A. Green, and D.A. Neumann, *J. Phys. Chem. Solids* **63**, 1779 (2002).
8. N. Mizutani, A. Kitazawa, O. Nobuyuki, and M. Kato, *J. Chem. Soc. (Jpn.) Ind. Ed.* **73**, 1097 (1970).
9. J.F. Mitchell, J.E. Millburn, M. Medarde, S. Short, and J.D. Jorgensen, *J. Solid State Chem.*, **141**, 599 (1998).
10. G.M. Veith, I.D. Fawcett, M. Greenblatt, and M. Croft, I. Nowik, *Int. J. Inorg. Mater.*, **2**, 2513 (2000).
11. L.J. Gillie, A.J. Wright, J. Hadermann, G. Tendeloo, and C. Greaves, *J. Solid State Chem*, **175**, 188 (2003).
12. M.S. Song, S.Y. Kim, and J.Y. Lee, *Ceramics Silikaty*, **48**(4), 175 (2004).
13. J.R. Carvajal, *Physiva*, **B192**, 55 (1993).
14. M.V. Lobanov, M. Greenblat, E.N. Caspi, J.D. Jorgensen, D.V. Sheptyakov, B.H. Toby, C.E. Botez, and P.W. Stephens, *J. Phys.: Condens. Matter*, **16**, 5339 (2004).
15. I.D. Fawcett, G.M. Veith, M. Croft, and I. Nowik, *J. Solid State Chem.*, **155**, 96 (2000).
16. P.D. Battle, W.R. Branford, A. Mihur, M.J. Rosseinsky, J. Singleton, J. Sloan, L.E. Spring, and J.F. Vente, *Chem. Mater.*, **11**, 674 (1999).
17. F. Prado and A. Manthiram, *J. Solid State Chem.*, **158**, 307 (2001).